

# **Civil Engineering Journal**

(E-ISSN: 2476-3055; ISSN: 2676-6957)

Vol. 11, No. 09, September, 2025



# A Study on the Impact of Crystalline Hydrophilic Additive and Microcapsules on Concrete Freeze-Thaw Durability

Anita Gojević <sup>1</sup>, Ivanka Netinger Grubeša <sup>2\*</sup>, Marijana Hadzima-Nyarko <sup>3</sup>

<sup>1</sup> City of Osijek, Franje Kuhača 9, 31000 Osijek, Croatia.

<sup>2</sup> Department of Construction, University North, 42 000 Varaždin, Croatia.

<sup>3</sup> Faculty of Civil Engineering and Architecture Osijek, University of J.J. Strossmayer of Osijek, 31 000 Osijek, Croatia.

Received 18 May 2025; Revised 22 August 2025; Accepted 26 August 2025; Published 01 September 2025

#### **Abstract**

This paper evaluates the effectiveness of a crystalline hydrophilic additive and chemical microcapsules in enhancing concrete's freeze-thaw resistance at both material and structural levels. Three concrete mixes were tested: a reference mix, one with the crystalline additive and one with microcapsules. Cubic specimens were tested for compressive strength, water absorption and relative dynamic modulus of elasticity before, after and during 56 freeze-thaw cycles (according to CEN/TR 15177). The reinforced concrete beams underwent the same freeze-thaw regime and were tested under displacement-controlled cyclic loading to evaluate residual capacity and serviceability. Although both additives improved freeze-thaw resistance, beams with the microcapsule performed better on most criteria, including increased stiffness (+14%), load-bearing capacity (up to +22%) and ductility after freeze-thaw loading. Notably, all mixes showed an unexpected increase in compressive strength after cycling. Although the microcapsules provided the best overall performance, the crystalline additive was more effective in reducing water absorption. The study highlights the practical applicability of microcapsules for structural elements and demonstrates their potential to improve performance properties under harsh environmental conditions. The research novelty lies in the dual-level evaluation – material and structural – and the systematic comparison of two innovative additives, allowing a more comprehensive understanding of their performance under freeze-thaw conditions.

Keywords: Reinforced Concrete Beams; Freezing-Thawing; Relative Dynamic Modulus of Elasticity; Water Absorption; Compressive Strength; Load-Bearing Capacity; Serviceability.

#### 1. Introduction

The longevity of buildings is predominantly influenced by the durability of the materials utilized in their construction. A critical factor that undermines this durability is the freeze-thaw cycle [1]. When temperatures drop below freezing, water within the material undergoes a phase transition, freezing and expanding, thereby exerting internal pressure on the material structure [2]. Repeated freeze-thaw cycles exacerbate this pressure, leading to a progressive deterioration of the material and a subsequent reduction in its overall durability. In cement-based composites, such deterioration manifests in surface scaling or the development of internal cracks [3].

One widely used method for enhancing concrete durability under freeze-thaw conditions is the incorporation of air-entraining agents into the concrete mixture [4]. These agents generate air voids during mixing, which disrupt capillary channels and reduce water penetration into the concrete. Lowering the water content in the concrete further helps to mitigate freeze-thaw damage. However, the use of air-entraining agents must be carefully controlled, as they can

<sup>\*</sup> Corresponding author: inetinger@unin.hr





© 2025 by the authors. Licensee C.E.J, Tehran, Iran. This article is an open access article distributed under the terms and conditions of the Creative Commons Attribution (CC-BY) license (http://creativecommons.org/licenses/by/4.0/).

negatively impact the compressive strength of the concrete [5]. In addition to air-entrainment, research has shown that concrete durability can be improved through the use of various mineral additives, such as slag [6], fly ash [7], and silica fume [8]. Other strategies include partial replacement of aggregate with rubber particles [9–12], incorporation of polymer binders [13, 14], polymer modification [15–17] or impregnation [18, 19], the use of superplasticizers [20], biomimetic polymer additives [21], polymer fibers [22], crystalline additive [23, 24], and chemically synthesized microcapsules [23, 25].

Researchers utilize various standardized methods to test the concrete's resistance to freezing and thawing cycles. For instance, Nicula et al. [6] uses the SR 3518 standard [26], while Saeed [18] applies the ASTM C666/C666M-15 standard, procedure A [27]. The GBT 50082 standard [28] is utilized by authors in studies [4, 17, 19, 20, 22, 25], and the ASTM C666/C666M-03(2008) standard, procedure A [29], is employed by authors in papers [7, 8, 12, 14, 21]. Kumar and Dev [10] adopt ASTM C666/C666M-03(2008), procedure B [29] while Chen et al. [30] adopt a combination of ASTM C666-15, procedure B and GBT 50082 standard. Meanwhile, the CEN/TS 12390-9 standard [31] is used by authors in papers [15, 16, 23, 24], and CEN/TR 15177 [32] is applied by authors in studies [16, 24].

Researchers assess concrete's resistance to freeze-thaw cycles using various parameters, including visual appearance [10, 30], changes in dynamic modulus [4, 6, 8, 11, 12, 16, 17, 21, 33], weight change [4, 7, 10, 12, 14, 15, 16, 18, 19, 20, 23, 24, 25, 33], volume change [7, 12, 21], changes in compressive or flexural strength [7, 10, 12, 14, 20, 22, 25], changes in permeability coefficient [7], ultrasonic pulse velocity [10, 12, 24], and pore size distribution [30].

Standardized methods exist for testing concrete's freeze-thaw resistance and monitoring specific parameters during these cycles. However, the behaviour of reinforced concrete under freeze-thaw conditions remains not yet comprehensively standardized and warrants further investigation. The high cost of specialized chambers for such testing has limited studies on the freeze-thaw resistance of concrete elements. Only a few research groups have addressed this issue, each employing distinct freeze-thaw regimes. Studies [34-39] examine the impact of freeze-thaw cycles on various properties of reinforced concrete beams. In their research, Qin et al. [34] constructed reinforced concrete columns with  $200 \times 200 \times 1100$  mm dimensions, saturated them with water at two months of age and subjected them to freeze-thaw cycles as outlined in GBT 50082 2009 [28]. These columns were anchored in a reinforced concrete foundation and loaded at the top to simulate a horizontal earthquake force. The authors concluded that exposure to freeze-thaw cycles significantly reduced the columns' load-bearing capacity, ductility, strength, and stiffness. Kosior-Kazberuk & Wasilczyk [35] investigated the behaviour of reinforced concrete beams measuring  $80 \times 120 \times 1100$  mm under two conditions: simultaneous exposure to single-point bending and freeze-thaw cycles and single-point bending alone. Each freeze-thaw cycle ranged in temperature from -20 °C to +20 °C. Over 150 cycles, the researchers monitored crack count, average crack width, beam deflection, and tensile-zone strain. Beams exposed to both bending and freeze-thaw cycles exhibited significantly higher crack count and width, as well as increased deflection and strain in the tensile zone, compared to beams subjected solely to bending.

Duan et al. [36] studied the behavior of reinforced concrete beams ( $80 \times 120 \times 1100$  mm) exposed to freeze-thaw cycles and then loaded to 0 %, 20 %, and 50 % of their ultimate load capacity in two-point bending. For comparison, they also tested a beam that had not been subjected to freeze-thaw cycles before loading. Beams exposed to freeze-thaw cycles and pre-loading underwent up to 80 freeze-thaw cycles, each involving a temperature change from -18 °C to 14 °C. The study concluded that the beams' ultimate load capacity decreased as a result of exposure to freeze-thaw cycles and increased levels of pre-loading. Gong et al. [37] conducted a similar test on reinforced concrete beams measuring  $150 \times 250 \times 2000$  mm, using the same freeze-thaw cycle regimen and preloading percentages as those in Duan et al. [36]. Preloading was applied at two points within the freeze-thaw chamber, and beams were subsequently tested in two-point bending. The results supported previous findings indicating that combined exposure to both freeze-thaw cycles and preloading significantly impact beam integrity more than either condition alone.

Cao et al. [38] examined the shear behaviour of reinforced concrete beams ( $150 \times 250 \times 2000$  mm) subjected to up to 150 freeze-thaw cycles. Although specific details of the cycles were not provided, the authors concluded that freeze-thaw exposure did not alter the beams' failure mechanism. Chen et al. [39] investigated the damage in reinforced concrete beams measuring  $120 \times 120 \times 600$  mm exposed to 150 freeze—thaw cycles according to the GBT 50082 standard, both without and with sustained load. These group of authors concluded that the sustained load further aggravates the damage to the elements, as measured by weight loss, reduction in dynamic modulus of elasticity, and load-bearing capacity. In addition to the previously mentioned studies addressing the issue of freeze—thaw effects on reinforced concrete structural elements, the authors in Liu et al. [40] and Yang et al. [41] also discuss freeze—thaw action in reinforced concrete elements; however, their elements are significantly smaller in size, with dimensions of  $150 \times 150 \times 150$  mm. Liu et al. [40] found that in reinforced concrete specimens of  $150 \times 150 \times 150$  mm size exposed to freeze—thaw cycles under the GBT 50082 regime, the bond between reinforcement and concrete drastically deteriorates under cyclic loading, and that this degradation is more strongly influenced by freeze—thaw cycles than by cyclic loading alone. Yang et al. [41], in a similarly designed study, further concluded that the effect of freeze—thaw cycles on the bond between reinforcement and concrete becomes more severe as the concrete's porosity increases and its density decreases.

Only a few studies [42-44] have examined how modifications to the concrete mix or structural elements influence the freeze-thaw resistance of reinforced concrete elements. Notably, Cao et al. [42] investigated reinforced concrete beams measuring  $100 \times 150 \times 1000$  mm, constructed with varying reinforcement and two concrete strengths (40 and 50 N/mm²). These beams were subjected to two-point bending after undergoing up to 125 freeze-thaw cycles, with each cycle involving immersion in water at temperatures ranging from -17  $\pm$  2 °C to 6  $\pm$  2 °C for 3 hours. The researchers found that both the load at which cracks first appeared and the ultimate load capacity decreased as the number of freeze-thaw cycles increased, though this effect was less pronounced for beams with higher concrete strength. They concluded that high-strength concrete can mitigate freeze-thaw effects in real-world exposure conditions.

Kim et al. [43] simultaneously investigated the impact of freeze—thaw cycles on both the material properties and reinforced concrete beams, using concrete mixes containing 0%, 0.15%, and 0.75% air-entraining agent by cement mass. At the material level, they prepared cylindrical specimens with a diameter of 100 mm and a height of 200 mm, subjecting them to freeze—thaw cycles under two different regimes. The first regime followed the standard ASTM C666-15, Procedure A [27], while the second involved the same freezing process as in the first regime, but with thawing in air instead of water. At the same time, reinforced concrete beams measuring  $100 \times 200 \times 1800$  mm were produced and exposed to freeze—thaw cycles according to the second (air-thaw) regime. On the cylindrical specimens, these authors monitored strength change, relative dynamic modulus of elasticity, and durability index. For both treatment regimes, it was concluded that after 300 freeze—thaw cycles, the specimens with 0.15% air-entraining agent showed the best frost resistance across all monitored parameters. The load-bearing capacity and deflection of the reinforced concrete beams, both untreated and treated with 300 freeze-thaw cycles under the second regime, were tested. It was found that increasing the amount of air-entraining agent led to a decrease in the elastic stiffness of the beams at room temperature, which further decreased after exposure to freeze-thaw cycles, primarily due to the reduction in concrete compressive strength. The failure mechanism of the beams remained unchanged before and after exposure to the freeze-thaw cycles.

Omran & El-Hacha [44] examined real-scale reinforced concrete beams  $(200 \times 400 \times 5150 \text{ mm})$  in two series: each series included one unreinforced beam, and four beams reinforced with carbon fibers in the tension zone at different prestressing levels (0%, 20%, 40%, and 60% of the fibers' ultimate tensile strength). Series 1 was subjected to 500 freeze-thaw cycles, while Series 2 experienced 500 freeze-thaw cycles plus preloading at 47% of the ultimate load capacity of the beam with unstressed carbon fibers. Each cycle ranged from -34 °C to +34 °C with 75% relative humidity. In Series 2, beams with prestressed carbon fibers showed fiber separation during loading but exhibited fewer cracks in the tensile zone than beams with unstressed fibers.

The referenced studies cover either the impact of freeze—thaw cycles on concrete as a material or on reinforced concrete elements, but studies that examine the effects of freeze—thaw cycles on both are rare. To the best of the authors' knowledge, the only such study is the one conducted by Kim et al. [43]. However, in that study, the standard procedures used to assess concrete's resistance to freeze—thaw cycles were modified for the purpose of exposing reinforced concrete beams to freeze—thaw action. This study investigates the influence of crystalline hydrophilic additives and chemical microcapsules on the resistance of both concrete and reinforced concrete beams to freeze—thaw cycles, using the same standardized method.

# 2. Experimental Part

## 2.1. Characteristics of Concrete Mix Components

Three concrete mixtures were prepared: a reference mixture (R), a mixture containing a crystalline hydrophilic additive (M1), and a mixture incorporating chemical microcapsules (M2). Dolomite aggregate with a particle size range of 0–4 mm was used in all mixtures and its granulometric curve is presented in Figure 1. This fine aggregate was selected due to the small cross-sectional dimensions of the reinforced concrete beams tested, as well as the minimal concrete cover in these beams. The density of the dolomite, determined according to HRN EN 1097-6 [45], was 2780 kg/m³. A dolomite-type filler was used.

The cement used in all mixtures was CEM I 52.5 N, sourced from the Nexe manufacturer, with a density of 2960 kg/m³, as determined per HRN EN 196-6 [46]. The specific surface area of the cement was determined using the BET method, in accordance with HRN ISO 9277 [47], and was measured at 3.79 m²/g. All mixtures were prepared with potable tap water, maintaining a water-to-cement ratio (w/c) of 0.35. Additionally, each mixture included the superplasticizer Visco Crete 5380 I at a dosage of 1 % by mass of cement, with a density of 1.08 g/cm³.

Mixture M1 was produced with the crystalline hydrophilic additive Penetron Admix, manufactured by Penetra, at 1 % by mass of cement. The density of this additive, determined in accordance with HRN EN 1097-6 [45], was 2910 kg/m³, and its specific surface area, measured using the BET method as per HRN ISO 9277 [47], was 2.7 kg/m³. Mixture M2 was prepared by incorporating chemical microcapsules at 1% by mass of cement. The composition and production methods of these microcapsules as well as their appearance are detailed in Gojević et al. [23] and briefly summarized here. To synthesize the microcapsules, 10 g of paraffin beads were first weighed and heated to 75 °C until fully melted. Subsequently, 20 g of toluene diisocyanate (TDI) were added, and the mixture was stirred using a mechanical stirrer for

3 hours at a constant temperature of 75 °C and a rotation speed of 600 rpm. After heating was stopped, 100 cm³ of perfluorotributylamine (PFTBA) was introduced, leading to the formation of microcapsules. These were then separated by vacuum filtration and dried at 40 °C for 24 hours.

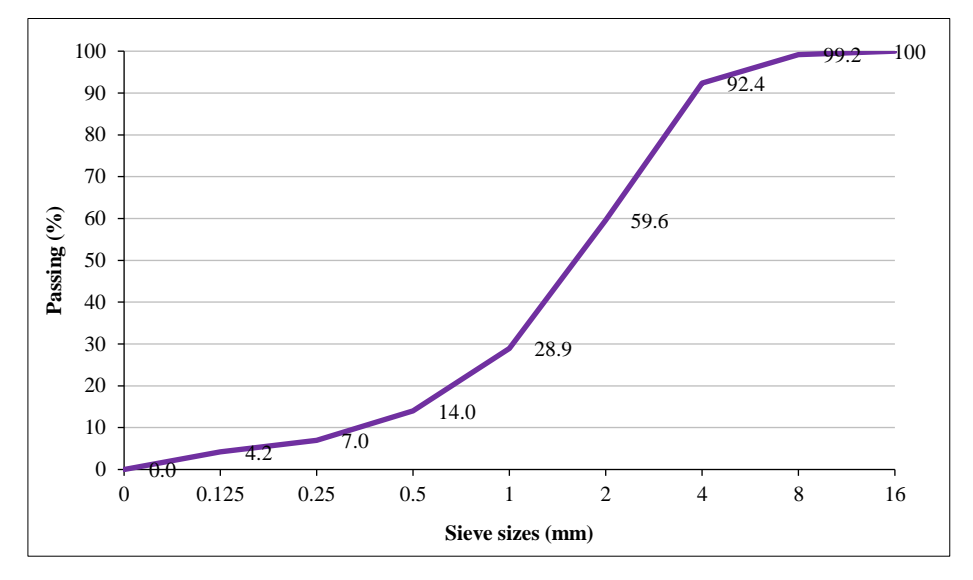


Figure 1. Granulometric curve of aggregate

#### 2.2. Composition of Concrete Mixtures

The compositions of the three concrete mixtures investigated are summarised in Table 1.

Mixture/Components	R	M1	M2
Cement (kg)	400	396	396
Water(kg)	140	140	140
w/c	0.35	0.35	0.35
Superplasticizer 1 % (kg)	4	4	4
Crystal hydrophilic additive 1 % (kg)	-	4	-
Microcapsules 1 % (kg)	-	-	4
Dolomite $0 - 4 \text{ mm (kg)}$	1864.94	1864.94	1864.94
Filler (kg)	98.16	98.16	98.16

Table 1. The composition of all concrete mixtures (per 1 m3 of concrete)

A laboratory mixer (DZ 100VS) was used to prepare the mixes. First, the aggregate, filler, and crystalline hydrophilic additive or chemical microcapsules were mixed for 1 minute. Next, cement was added and mixing continued for an additional 2 minutes. Finally, water containing the superplasticizer was introduced, and the mixture was blended for another 2 minutes, resulting in a total mixing time of 5 minutes.

# 2.3. Preparation of Test Samples

From each of the three concrete mixtures, nine cubic specimens (15 cm per side) were cast and cured by immersion in water for 28 days. These nine specimens were divided into three groups, as illustrated schematically in Figure 2.

The first group of three cubes was designated for determining the compressive strength at 28 days of age. The second group was subjected to 56 freeze-thaw cycles (referred to as "treated" specimens) exposure according to Clause 7 of CEN/TR 15177:2006 standard [32] using an ultrasonic pulse transmission time device. The third group was stored in the laboratory at room temperature as "untreated" specimens. Each freeze-thaw cycle lasted 12 hours, so the second group spent 28 days in the freeze-thaw chamber. Consequently, at the end of this regimen, these specimens were 56 days old. After completing 56 freeze-thaw cycles, both the "treated" (second group) and "untreated" (third group) cubes, aged 56 days, were tested for compressive strength. These results were used as input data for calculating the required reinforcement in the reinforced concrete beams. Another key input for this calculation the required beam reinforcement was the secant modulus of elasticity (Ecs), determined using Equation 1 from standard EN 1992-1-1:2023 [48]. The compressive strength at 56 days, obtained after freeze-thaw exposure for the treated samples or standard curing for the untreated samples—was employed in this calculation:

$$E_{cs} = 9500 \cdot \sqrt[3]{(f_{ck} + 8)}$$
 (1)

where  $f_{ck}$  is the characteristic compressive strength of concrete (in MPa).

The length of the reinforced concrete beams was limited by the dimensions of the freeze-thaw chamber; therefore, the total beam length was set to 100 cm. A cross-section of  $10 \times 10 \text{ cm}$  cross-section was chosen to ensure a ductile flexural failure during pure bending tests. The required reinforcement was determined through iterative numerical calculation (using Seismo Struct software), with control of the total vertical load and mid-span deflection of the beam element. All beams were reinforced with grade B500B steel: two 8 mm diameter bars in the tension zone, two 6 mm diameter bars in the compression zone (longitudinal reinforcement), and 6 mm stirrups spaced at 60 mm (transverse reinforcement). The concrete cover was maintained at 6 mm. A schematic representation of the beam reinforcement is provided in Figure 3.

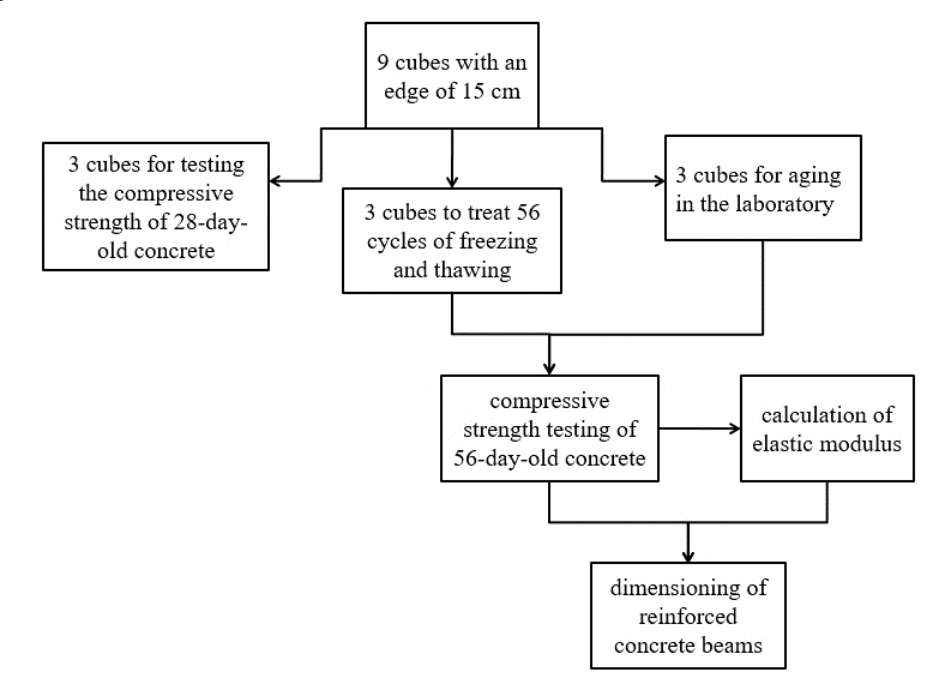


Figure 2. Distribution of concrete cubes for different tests

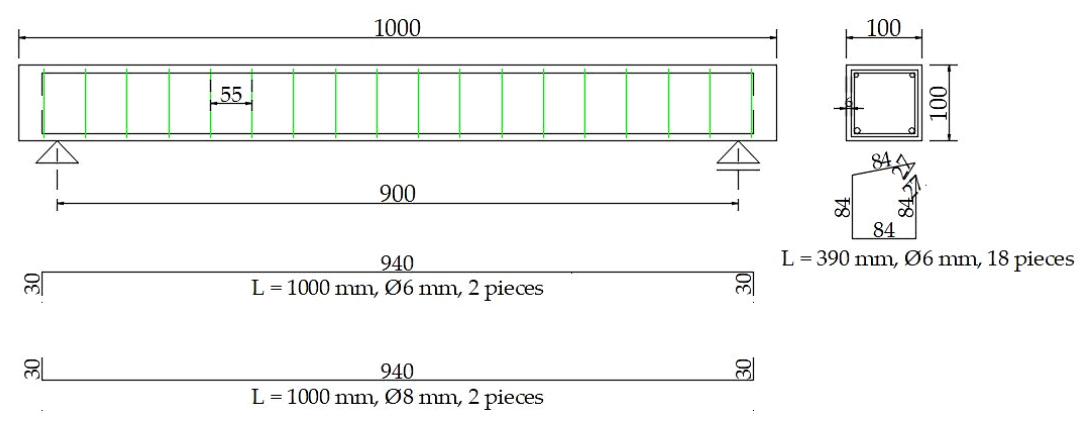


Figure 3. Schematic of longitudinal and transverse reinforcement for the beams

The concrete, prepared as described in Section 2, was cast into pre-assembled moulds with reinforcement cages (Figure 4). Four reinforced concrete beams were produced from each concrete mixture (Figure 5). The fresh concrete was compacted using vibrating poker.



Figure 4. Formwork and reinforcement cages for the producing the beams

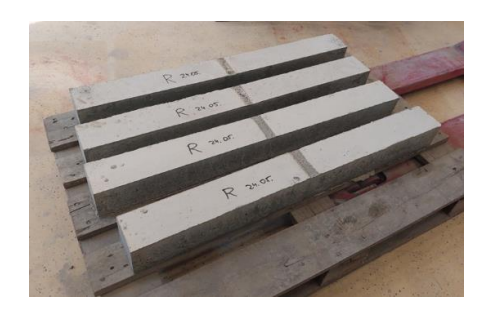


Figure 5. Reinforced concrete beams

The beams were cured in the laboratory using water-sprinkling until they reached 28 days of age.

## 2.4. Freeze-thaw Treatment Regime for Test Samples

The second group of cubes (designated for freeze-thaw exposure in Figure 2) underwent 56 freeze-thaw cycles in a chamber capable of absorbing and releasing water in accordance with Clause 7 of CEN/TR 15177:2006 [32]. Additionally, two of the four reinforced concrete beams from each mixture, at 28 days of age, were subjected to the 56-cycle freeze-thaw regimen in the chamber.

#### 2.5. Test Methods for Cubes and Reinforced Concrete Beams

During the freeze-thaw cycles, ultrasonic pulse velocity measurements were conducted to calculate the relative dynamic modulus of elasticity. Water absorption was also monitored in accordance with Clause 7 of CEN/TR 15177:2006 [32]. Upon completion of the freeze-thaw cycles, both treated and untreated cubes were tested for compressive strength in accordance with EN 12390-3:2019 [49]. After exposure of the reinforced concrete beams to freeze-thaw cycles (at 56 days of age), tests were performed to evaluate their residual load-bearing capacity and serviceability. The static scheme for the experimental testing of the beams is presented in Figure 6, while Figures 7-a and 7-b show the testing setup on the universal testing machine (Shimadzu).

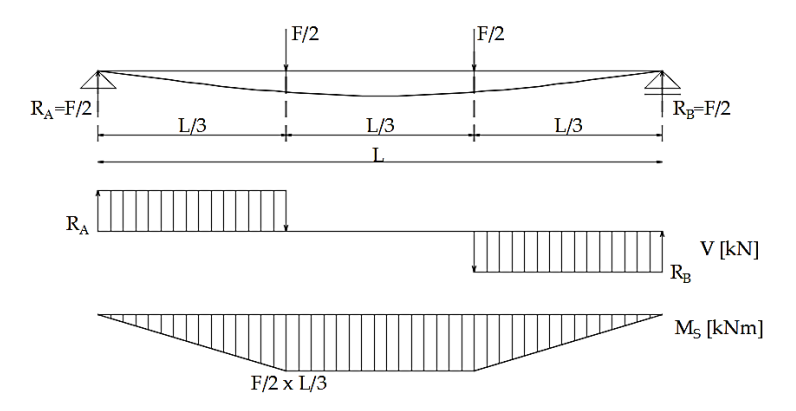


Figure 6. Static system for testing the reinforced concrete beams in bending





(b) side view

Figure 7. Bending test of a reinforced concrete beam using the Shimadzu universal testing machine

Three Linear Variable Differential Transformer (LVDT) sensors were used to measure deformations and vertical deflection of the beams. Their arrangement is shown schematically in Figure 8.

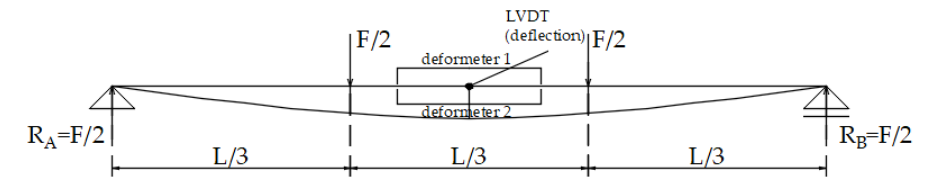


Figure 8. Position of measuring devices (LVDTs) on the beams

All specimens were exposed to cyclic, strain-controlled loading following the procedure recommended by FEMA 461 in 2007 [50]. The loading process involved a series of repetitive cycles with incrementally increasing amplitude, where each step was increased by a factor of 1.4. Each displacement level amplitude was subjected to two loading cycles. The secant stiffness, ductility  $\mu_1$  and  $\mu_2$ , maximum force and deflection at maximum force, and failure force and deflection at failure force were measured during the tests.

#### 2.6. Test Results for Cubes and Reinforced Concrete Beams

## 2.6.1. Results of Non-destructive Testing Methods for Cubes and Reinforced Concrete Beams

Figure 9 presents the variation in the relative dynamic modulus of elasticity of the cube specimens during the freeze-thaw cycles. Figure 10 depicts water absorption throughout the freeze-thaw cycles. Each curve represents the average of three measurements, with a standard deviation of up to 10 %.

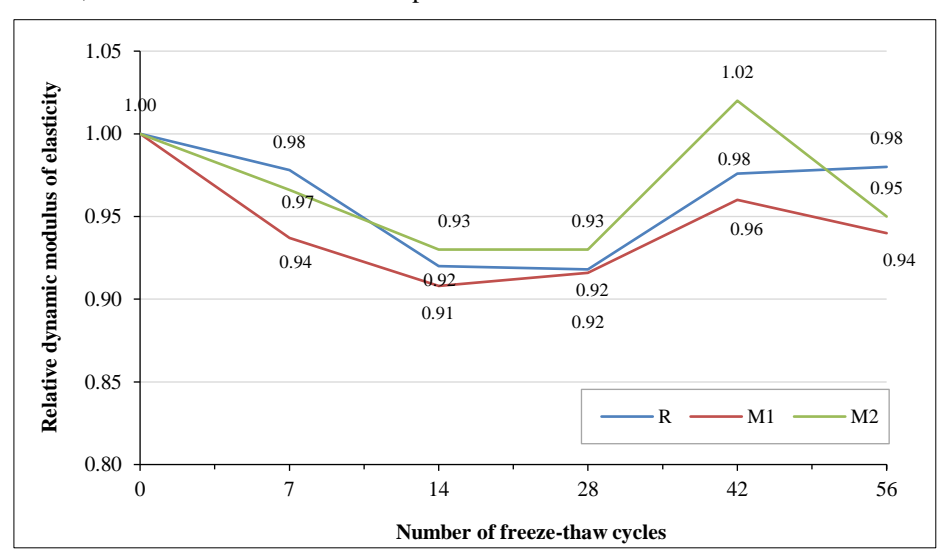


Figure 9. Change in the relative dynamic modulus of elasticity of cubes during freeze-thaw cycles

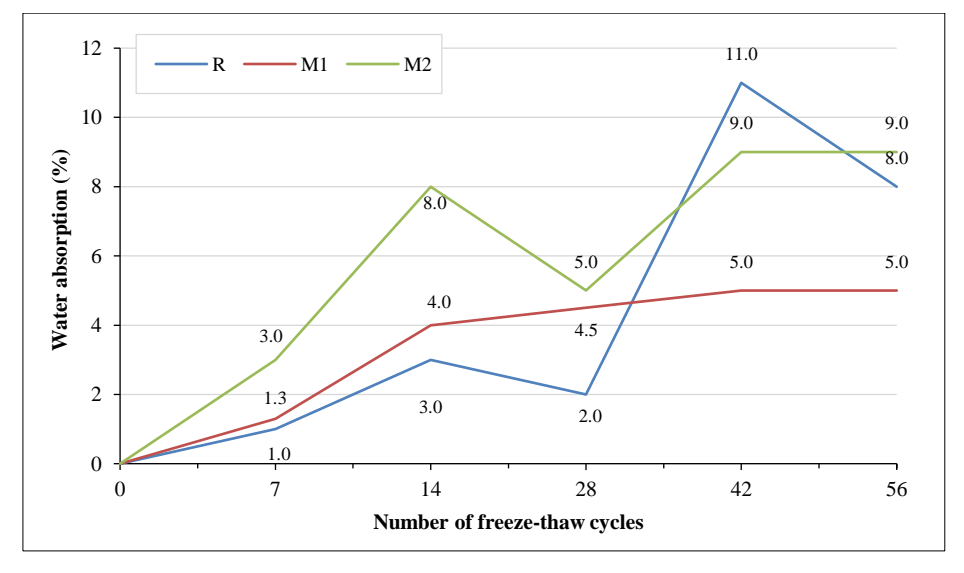


Figure 10. Water absorption of cubes during freeze-thaw cycles

# 2.6.2. Results of Destructive Methods of Testing Blocks and Reinforced Concrete Beams

Table 2 shows the compressive strength of 28-day-old cubes (three specimens per mixture). The values represent the averages of three tests, accompanied by their standard deviations.

Table 2. Compressive strength of 28-day-old cubic specimens

Mixture	R	M1	M2
	49.00	57.79	49.26
Compressive strength (MPa)	49.17	56.54	54.70
	53.00	60.16	50.69
Mean value of compressive strength (MPa)	50.39	58.16	51.55
Standard deviation	2.26	1.84	2.82

Tables 3 and 4 present the compressive strength data for concrete cubes subjected to different conditions. Table 3 reports the compressive strengths of cubes exposed to freeze-thaw cycles ("treated"), whereas Table 4 presents the strengths of cubes maintained at room temperature ("untreated"). All values represent the means of three tests, with accompanied by their respective standard deviations.

Table 3. Compressive strength of cubes after 56 freeze-thaw cycles ("treated")

Mixture	R	M1	M2
	69.74	78.78	66.66
Compressive strength (MPa)	67.31	73.75	65.73
	72.69	77.47	66.00
Mean value of compressive strength (MPa)	69.91	76.67	66.13
Standard deviation	2.69	2.61	0.48

Table 4. Compressive strength of cubes kept in the laboratory at room temperature ("untreated")

Mixture	R	M1	M2
	64.20	65.30	62.06
Compressive strength (MPa)	62.94	65.02	65.09
	65.18	70.99	60.83
Mean value of compressive strength (MPa)	64.11	67.10	62.66
Standard deviation	1.12	3.37	2.19

The static modulus of elasticity required for beam design was determined using Equation 1, based on the mean compressive strengths given in Tables 3 and 4. The calculated values are presented in Tables 5 and 6.

Table 5. Calculated static modulus of elasticity (treated concrete, after freeze-thaw cycles)

Mixture	R	M1	M2
The mean value of the static modulus of elasticity of the treated concrete (MPa)	40575.22	41715.21	39907.54

Table 6. Calculated static modulus of elasticity (untreated concrete)

Mixture	R	M1	M2
The mean value of the static modulus of elasticity of untreated concrete (MPa)	39541.1	40081.44	39274.88

The extent of damage to the concrete mixes during the freeze-thaw cycles, expressed as the ratio of the compressive strengths of "treated" (Table 3) and "untreated" cube samples (Table 4), is shown in Figure 11. In the figure, label "A" denotes the treated samples subjected to freeze-thaw cycles, while label "B" corresponds to the untreated samples maintained at room temperature.

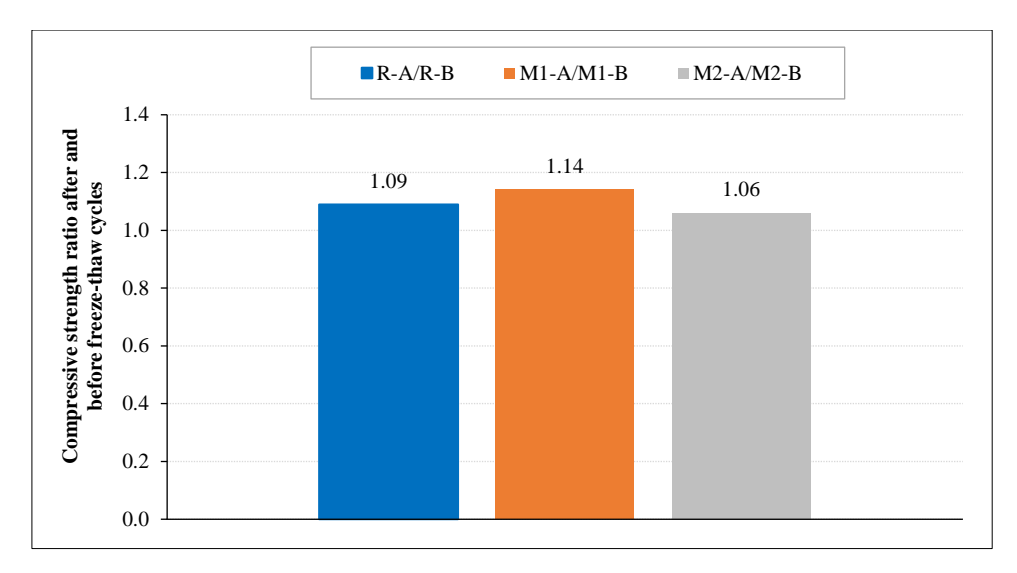


Figure 11. The ratio of compressive strengths of freeze-thaw treated cubes vs. untreated cubes

A typical failure mode of reinforced concrete beams under bending is shown in Figure 12 during the load-bearing capacity test.



Figure 12. The failure mode of a beam in pure bending

Figure 13 shows the mean load-deflection curves for all untreated and treated beams. The label "A" again denotes treated beams, while the label "B" corresponds to the untreated beams. Each curve represents the average of the two beams fabricated from the same concrete mixture.

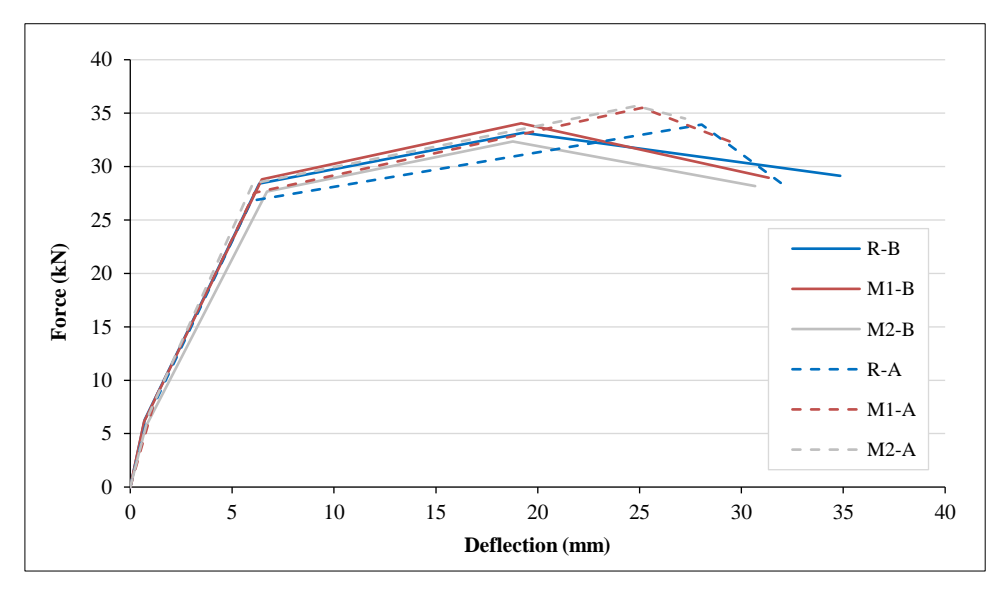


Figure 13. Relationship between total force and mid-span deflection for reinforced concrete beams - mean curves (for all three mixtures, before and after freeze-thaw cycles)

Due to the nonlinear behavior exhibited by the beams, Figure 14-a presents the absolute secant stiffness ( $k_{sec}$ ), whereas Figure 14-b illustrates the ratio of secant stiffness between treated and untreated beams.

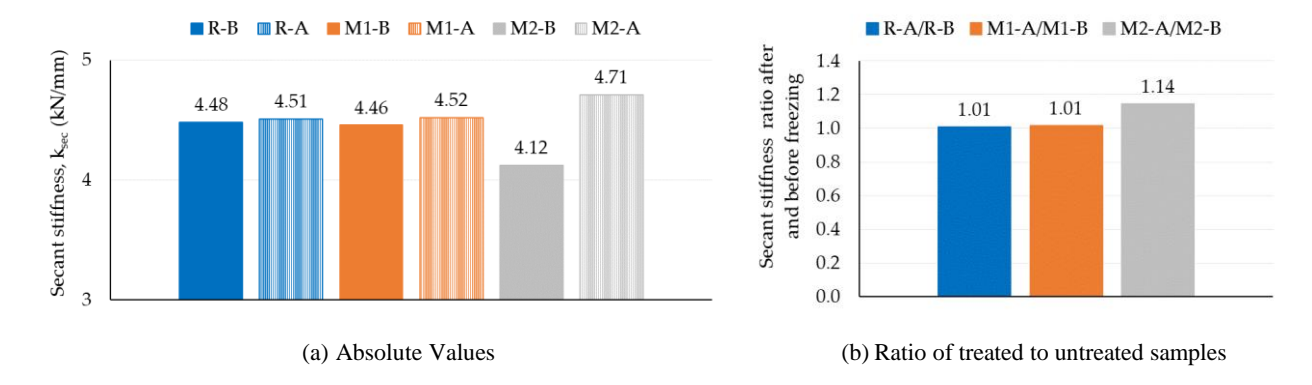


Figure 14. Secant stiffness (ksec) for reinforced concrete beams

An important property of reinforced concrete beams is their ductility, i.e. their ability to withstand plastic deformation up to the moment of failure, which is important for the possibility of prediction. Ductility ( $\mu_1$ ) is defined as the ratio of the deflection at maximum beam strength ( $d_{max}$ ) to the deflection at yield of the main tensile reinforcement ( $d_y$ ). Figure 15-a shows the  $\mu_1$  values for treated and untreated beams, while Figure 15-b shows their ratios.

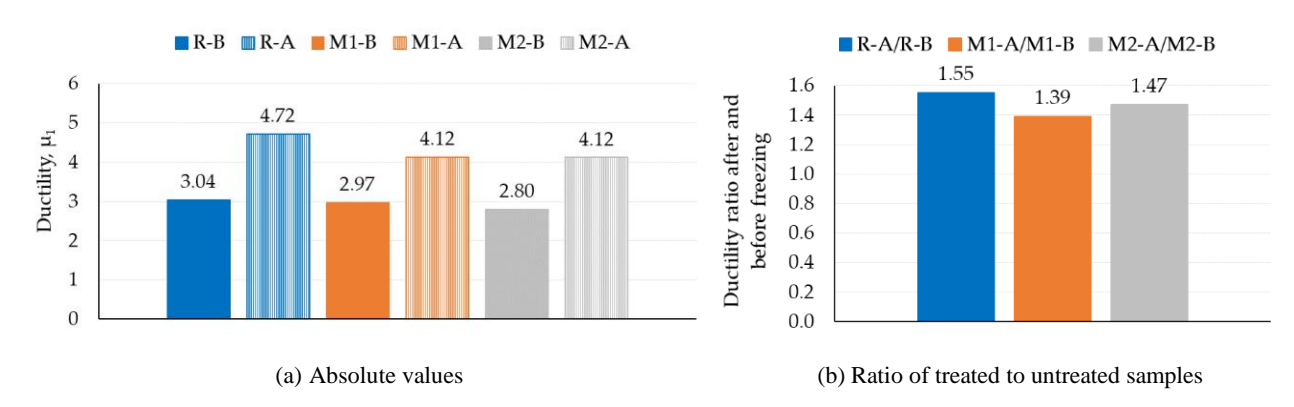


Figure 15. Ductility  $(\mu_1)$  for reinforced concrete beams

Ultimate ductility ( $\mu_2$ ) is defined as the ratio of deflection at ultimate beam capacity ( $d_u$ ), which corresponds to the point of complete loss of load-bearing capacity, to the deflection at yield of the main tensile reinforcement ( $d_y$ ). Figure 16-a presents the  $\mu_2$  values for the tested beams, while Figure 16-b shows their ratios.

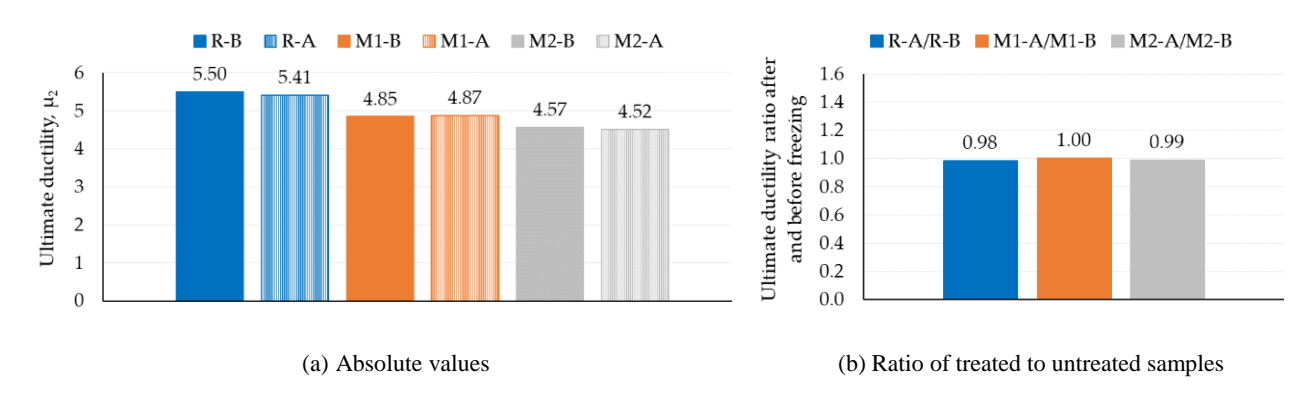


Figure 16. Ultimate ductility  $(\mu_2)$  for reinforced concrete beams

Figure 17-a presents the maximum forces ( $F_{max}$ ) reached by treated and untreated beams, and Figure 17-b shows their ratios.

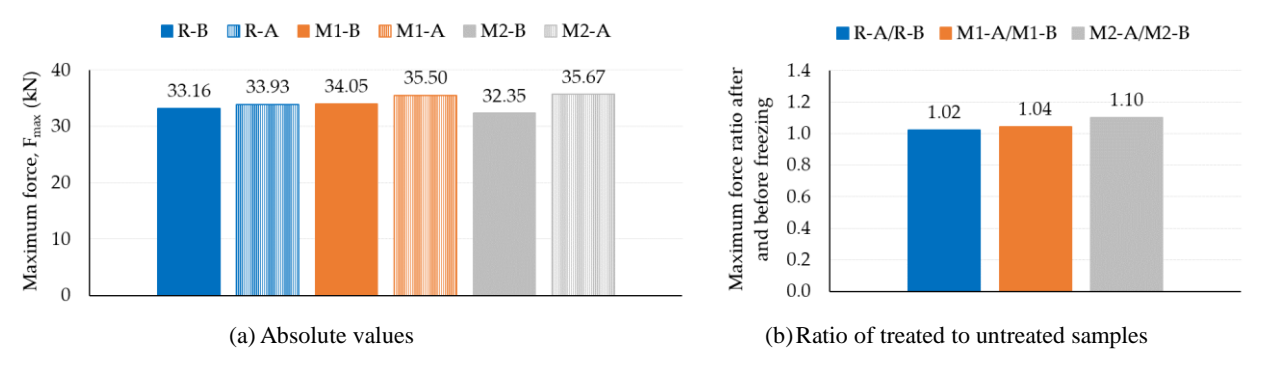


Figure 17. Maximum forces for reinforced concrete beams

Figure 18-a presents the deflection at the maximum force  $(d_{max})$  for both treated and untreated beams, while Figure 18-b illustrates their corresponding ratios.

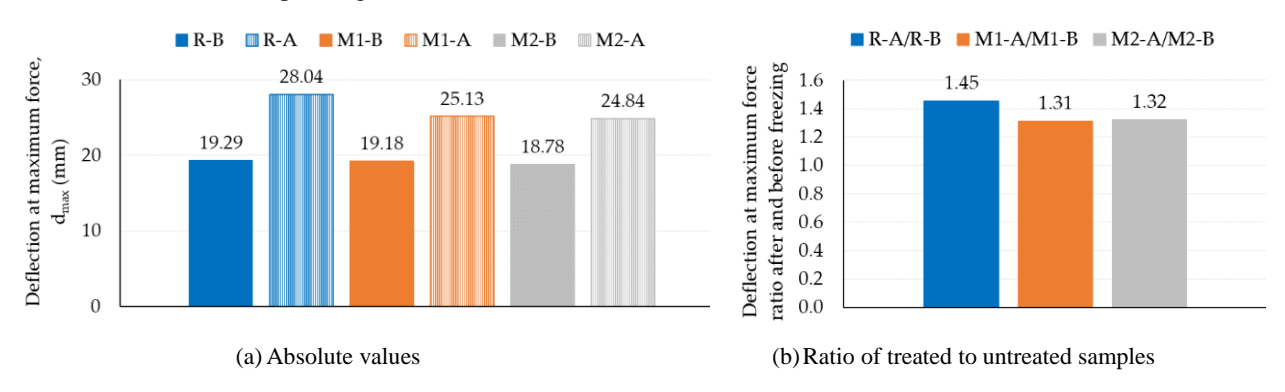


Figure 18. Deflections at maximum force for reinforced concrete beams

Figure 19-a shows the load (force) at failure (F<sub>u</sub>) for treated and untreated beams, with Figure 19-b depicting the respective ratios.

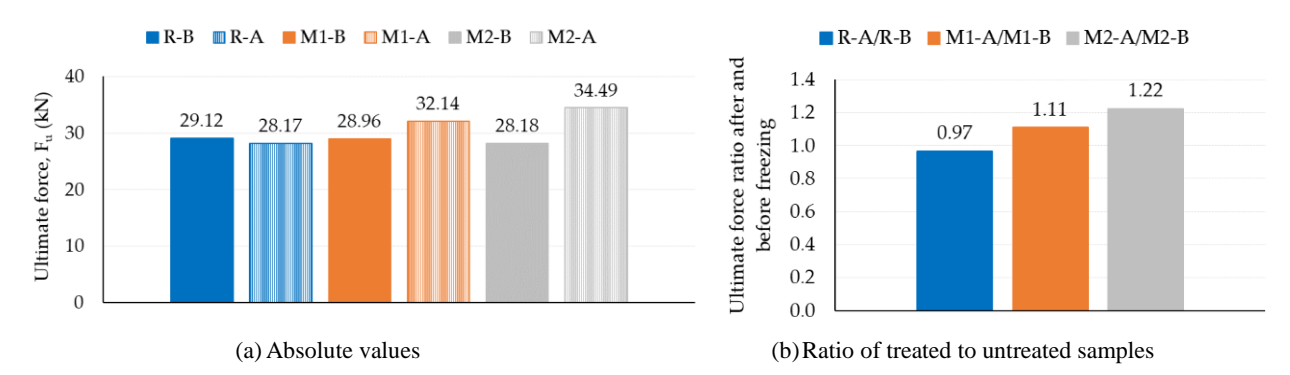


Figure 19. Forces at failure for reinforced concrete beams

Finally, Figure 20-a shows the deflection at failure  $(d_u)$  for treated and untreated beams, and Figure 20-b presents their ratios.

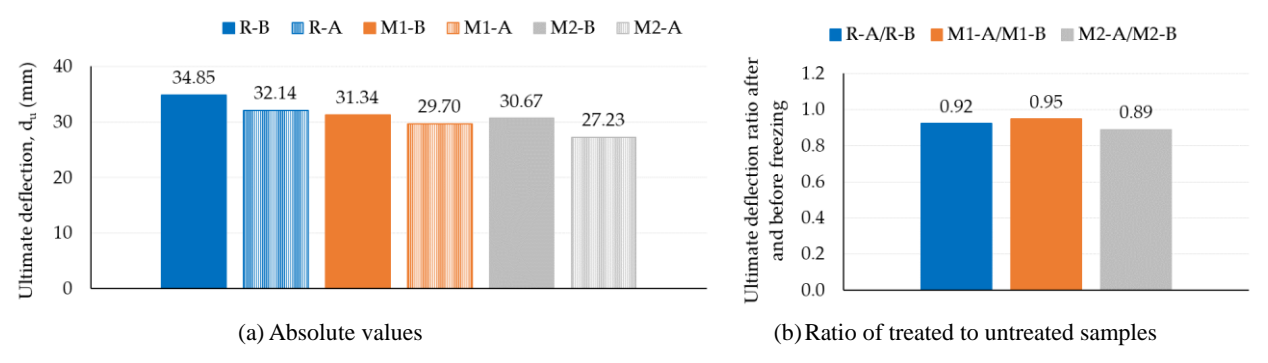


Figure 20. Deflections at failure for reinforced concrete beams

## 3. Discussion

Among the cube specimens, the relative dynamic modulus of elasticity showed the most significant decrease with increasing freeze-thaw cycles in mixture M1 (6%), followed by the reference mixture M2 (5%). In contrast, mixture R exhibited the smallest decrease (2%) in this modulus (Figure 9), suggesting R has the highest freeze-thaw resistance based on this parameter. However, the water absorption tests (Figure 10) revealed a different trend: mixture M2 had the highest absorption after 56 freeze-thaw cycles (9%), implying the worst freeze-thaw resistance if considered in isolation. Conversely, mixture R performed somewhat better (8% of water uptake), and M1 showed the smallest increase in water absorption (5%), indicating the best freeze-thaw resistance according to this measure. Crystalline hydrophilic additives (M1) contributed positively to the compressive strength of the 28-day-old concrete, whereas the microcapsules (M2) did not exhibit such an effect, as shown in Table 2. A similar conclusion can be drawn from the data in Tables 3 and 4.

However, it is noteworthy that freeze-thaw exposure resulted in an increase in the compressive strength of all mixtures, which contrasts with previous findings [25], where a decrease was observed. This can be attributed to the fact that the test specimens are still in the phase of strength development, and the presence of water contributes more to the increase in strength than the freeze—thaw cycles contribute to its deterioration. While Du et al. [25] concluded that adding 1 % microcapsules positively affects the residual compressive strength of concrete, this result was not confirmed in the present study. As shown in Figure 11, all mixtures actually exhibited increased compressive strengths after freeze-thaw cycles (6-14% of increase), with the largest increase observed in mixture M1 (14%). These trends are directly reflected in the calculated moduli of elasticity presented in Tables 5 and 6. Let us recall that it was mixture M1 that showed the greatest drop in the dynamic modulus of elasticity (Figure 9), so such a good result in the compressive strength ratio after and before freezing was not expected. However, it can be explained through the conclusion of the study conducted in Park et al. [51], which states that ultrasonic pulse velocity results show little correlation with compressive strength results

Certain conclusions can be drawn from the relationship between displacement and deflection with regard to the loadbearing capacity and the post-elastic behavior of the element (Figure 13). The relationship is linear for almost all beams at a similar value of about 6 kN. Then the yielding of the reinforcing steel occurs (reaching and exceeding the yield strength of the main tensile (longitudinal) reinforcement), which is again almost the same for all beams (from 25 to 28 kN). The differences are less than 10%. The greatest differences occur in the maximum force achieved and the associated displacement, which is the most important, as the element then breaks. Beam M1 shows the highest maximum force achieved (34.04 kN), which is greater than the maximum force of the reference beam (33.16 kN). More importantly, the freeze-thaw treated beams show both a higher maximum force and a higher deflection than the untreated samples. Figure 13 shows that the highest load-bearing capacity after freeze-thaw exposure was observed in beams made of concrete mixture M2, followed by M1, and then the mixture R. Notably, all beams exhibited increased maximum forces after 56 freeze-thaw cycles, which contradicts the findings reported in Qin et al. [34] and Duan et al. [36], where freeze-thaw cycles were shown to reduce load-bearing capacity, stiffness, and ductility. However, the results in Figure 13 are consistent with the date on compressive strength in Figure 11, which increase due to exposure to freeze-thaw cycles, subsequently leading to a rise in the maximum forces achieved by the beams after freezing and thawing. Secant stiffness is important because it allows the evaluation of the overall stiffness of a structural element at larger deformations when the linear (elastic) relationship between force and deflection no longer applies. It is defined here as the ratio of force to deformation in extension (Fy/dy).

As can be seen in Figure 14-a, the secant stiffness values have similar values for all treated and untreated beams, except for the beams with concrete incorporating chemical microcapsules (M2). According to the results shown in Figure 14-b, the freeze-thaw treatment had no effect on the change in secant stiffness of the reinforced concrete beams made with the reference mixture (R) and the mixture containing the crystalline hydrophilic additive (M1), but it significantly affected the mixture containing microcapsules (M2). The addition of microcapsules (M2) decreased the secant stiffness of the untreated reinforced concrete beams (Figure 14-a) compared to the untreated reference beam; however, the freeze-thaw cycles had a positive effect, increasing the secant stiffness of the beam by 14% (Figure 14-b). In general, the freeze-thaw cycles positively affect the secant stiffness.

Figures 15-a and 15-b show the ductility  $\mu_1$ . All three mixtures exhibited higher ductility  $\mu_1$  in their treated beams compared to the untreated ones; the relative increases were 55 % for R, 47 % for M2, and 39 % for M1. Under this freeze-thaw regime, ductility  $\mu_1$  increased across all tested beams. The decrease in the dynamic modulus of elasticity of concrete cube specimens due to freeze-thaw cycles, as shown in Figure 9, was expected to result in increased ductility of the beams after exposure. The greatest reduction in the dynamic modulus (Figure 9) was observed in mixture M1, so the highest increase in ductility was reasonably expected in this mixture. However, this was not the case; the greatest increase in ductility was observed in the beam made from mixture R. When it comes to ductility values  $\mu_2$ , it can be said that both types of additives caused a decrease in ductility  $\mu_2$  in the untreated beams compared to the untreated reference beam (Figure 16-a). However, the ductility ratios of the beams before and after freezing (Figure 16-b) show that the ductility of all beams remained practically unchanged after exposure

to freeze-thaw cycles. As shown in Figure 17-a, the maximum forces achieved by untreated beams were relatively similar across all mixtures. However, following freeze-thaw cycles, these forces increased—approximately 10 % for M2, 4 % for M1, and 2 % for R (Figure 17-b).

Although the differences are not large, they are sufficient to allow greater deflection before reaching the concrete's compressive strength limit, thereby resulting in significantly increased ductility in the treated beams. As shown in Figures 18-a and 18-b, the largest increase in deflection at maximum load due to freeze-thaw cycles occurred in the reference mixture R (45 %), followed by M1 (31 %) and M2 (32 %). With respect to the load at failure (Figure 19-a), the beams from mixtures R, M1, and M2 showed comparable values in the untreated state. However, after freeze-thaw cycles, the load at failure increased by 11 % for M1 beams and 22 % for M2 beams, while R beams experienced a slight decrease of 3 % (Figure 19-b). These findings suggest that freeze-thaw cycles may be beneficial for beams with crystalline or microcapsule additives. Figures 20-a and 20-b indicate that the deflection at failure was actually reduced by freeze-thaw cycles across all mixtures, although the magnitude of this reduction varied among them. Additionally, the crystalline or microcapsule additives further contributed to decreased failure deflections. In general, higher-strength concretes also exhibit proportionally higher moduli of elasticity (Tables 3 to 6). Therefore, it is not surprising that treated beams of mixture M2, which achieved the highest compressive strengths, also demonstrate the highest moduli of elasticity, resulting in the greatest load-bearing capacity and relatively lower deflection compared to the other beams.

# 4. Conclusions

The effectiveness of crystalline hydrophilic additives and chemical microcapsules in improving the freeze-thaw resistance of concrete was evaluated through a series of tests performed on concrete cubes and reinforced concrete beams. Table 7 provides a ranking of each mixture (1 = best, 3 = worst) based on various measured properties

Table 7. Summary of the effectiveness of each concrete mixture and its reinforced concrete beams across all methods

	Tested property/mixture	R	M1	M2
t nts ss	Relative dynamic modulus of elasticity after 56 cycles	1	3	2
Indirect assessments on cubes	Water absorption of cubes after 56 cycles	2	1	3
Inc asses	Ratio of compressive strength (treated vs. untreated cubes)	2	1	3
<i>r</i> )	Ratio of secant stiffness (treated vs. untreated beams)	2/3	2/3	1
Direct assessments on RC beams	The ratio of ductility $\mu_1$ (treated vs. untreated)	1	3	2
ents c	The ratio of ultimate ductility $\mu_2$ (treated vs. untreated)	1/2/3	1/2/3	1/2/3
essme	Ratio of maximum forces (treated vs. untreated)	3	2	1
asse b	Ratio of deflection at max force (treated vs. untreated)	3	1/2	1/2
irect	Ratio of force at failure (treated vs. untreated)	3	2	1
Д	Ratio of deflection at failure (treated vs. untreated)	2	3	1
	Summary of rankings	3×1; 4×2; 3×3	4×1; 3×2; 3×3	6×1; 2×2; 2×3

Table 7 shows that, regarding the relative dynamic modulus of elasticity, the results rank mixture R as having the greatest resistance to freeze-thaw cycles, with M2 and M1 following. Water absorption measurements rank M1 as the most resistant, with R and M2 ranked subsequently. Concerning the ratio of compressive strengths (freeze-thaw treated vs. untreated), mixture M1 demonstrates the best freeze-thaw resistance, followed by mixtures R and M2. The secant stiffness ratio is highest in mixture M2 and almost equal in mixtures M1 and R. Regarding the ductility ratio, the best performance was achieved by mixture R, followed by mixture M2, and then M1. In terms of ultimate ductility, no mixture stands out, as all concrete mixtures showed equal effectiveness. For the ratio of maximum forces, the most effective mixture was M2, followed by M1 and finally R. In terms of deflection ratio at maximum force (where lower deflection ratio indicates better performance), mixtures M1 and M2 proved to be more effective than mixture R. The ratios of forces at failure indicate that mixture M2 was the most effective, followed by M1 and R. The deflection ratios at failure (again, lower deflection indicates better performance) show that mixture M2 was the most effective, followed by mixtures R and M1. Overall, considering these ten parameters, mixture M2 demonstrated the best performance, ranking as the most effective in six out of ten measurements, followed by mixture M1, which ranked highest in four measurements, and mixture R, which ranked highest in three measurements.

The results lead to the conclusion that microcapsules provide greater effectiveness in enhancing concrete's freezethaw resistance than crystalline hydrophilic additives, although both additives improve freeze-thaw resistance. Nevertheless, due to cost considerations of both additives, the more affordable crystalline hydrophilic additive is preferable.

#### 5. Declarations

#### 5.1. Author Contributions

Conceptualization, A.G.; methodology, A.G. and I.N.G.; formal analysis, A.G.; investigation, A.G., I.N.G., and M.H.N.; resources, I.N.G.; writing—original draft preparation, A.G. and I.N.G.; writing—review and editing, M.H.N.; visualization, A.G. and I.N.G.; supervision, I.N.G. and M.H.N. All authors have read and agreed to the published version of the manuscript.

#### 5.2. Data Availability Statement

The data presented in this study are available on request from the corresponding author.

## 5.3. Funding

The results presented in this scientific paper have been obtained through the research activities within the projects "Circular economy in the construction industry" of University North, Croatia.

#### 5.4. Conflicts of Interest

The authors declare no conflict of interest.

## 6. References

- [1] Surej K. R. (1997). Evaluation and Improvement of Frost Durability of Clay Bricks. Ph.D. Thesis, Concordia University, Ottawa, Canada.
- [2] Pilehvar, S., Szczotok, A. M., Rodríguez, J. F., Valentini, L., Lanzón, M., Pamies, R., & Kjøniksen, A. L. (2019). Effect of freeze-thaw cycles on the mechanical behavior of geopolymer concrete and Portland cement concrete containing micro-encapsulated phase change materials. Construction and Building Materials, 200, 94–103. doi:10.1016/j.conbuildmat.2018.12.057.
- [3] Richardson, M. G. (2023). Fundamentals of Durable Reinforced Concrete. CRC Press, London, United Kingdom. doi:10.1201/9781003261414.
- [4] Qiu, Y., Peng, H., & Zhao, H. (2020). Study on New Type of Concrete Air-Entraining Agent. 2020 International Conference on Artificial Intelligence and Electromechanical Automation (AIEA), 807–810. doi:10.1109/aiea51086.2020.00176.
- [5] Nowak-Michta, A. (2019). Impact analysis of air-entraining and superplasticizing admixtures on concrete compressive strength. Procedia Structural Integrity, 23, 77–82. doi:10.1016/j.prostr.2020.01.066.
- [6] Nicula, L. M., Corbu, O., & Iliescu, M. (2020). Influence of blast furnace slag on the durability characteristic of road concrete such as freeze-thaw resistance. Procedia Manufacturing, 46, 194–201. doi:10.1016/j.promfg.2020.03.029.
- [7] Islam, M. M., Alam, M. T., & Islam, M. S. (2018). Effect of fly ash on freeze–thaw durability of concrete in marine environment. Australian Journal of Structural Engineering, 19(2), 146–161. doi:10.1080/13287982.2018.1453332.
- [8] Zhang, P., & Li, Q. F. (2014). Freezing-thawing durability of fly ash concrete composites containing silica fume and polypropylene fiber. Proceedings of the Institution of Mechanical Engineers, Part L: Journal of Materials: Design and Applications, 228(3), 241–246. doi:10.1177/1464420713480984.
- [9] Li, X., Ling, T. C., & Hung Mo, K. (2020). Functions and impacts of plastic/rubber wastes as eco-friendly aggregate in concrete

   A review. Construction and Building Materials, 240. doi:10.1016/j.conbuildmat.2019.117869.
- [10] Kumar, R., & Dev, N. (2022). Effect of acids and freeze—thaw on the durability of modified rubberized concrete with optimum rubber crumb content. Journal of Applied Polymer Science, 139(21), 52191. doi:10.1002/app.52191.
- [11] He, Y., Xu, F., & Wei, H. (2022). Effect of Particle Size on Properties of Concrete with Rubber Crumbs. American Journal of Civil Engineering, 10(3), 79–87. doi:10.11648/j.ajce.20221003.11.
- [12] Pham, N. P., Toumi, A., & Turatsinze, A. (2019). Effect of an enhanced rubber-cement matrix interface on freeze-thaw resistance of the cement-based composite. Construction and Building Materials, 207, 528–534. doi:10.1016/j.conbuildmat.2019.02.147.
- [13] Grubeša, I. N., Juradin, S., & Mrakovčić, S. (2024). Aging studies of polymer composites in freeze-thaw conditions. Aging and Durability of FRP Composites and Nanocomposites, 95–134, Woodhead Publishing, Sawston, United Kingdom. doi:10.1016/b978-0-443-15545-1.00003-2.
- [14] Jafari, K., Heidarnezhad, F., Moammer, O., & Jarrah, M. (2021). Experimental investigation on freeze-thaw durability of polymer concrete. Frontiers of Structural and Civil Engineering, 15(4), 1038–1046. doi:10.1007/s11709-021-0748-2.
- [15] Qu, Z., Guo, S., Sproncken, C. C. M., Surís-Valls, R., Yu, Q., & Voets, I. K. (2020). Enhancing the Freeze–Thaw Durability of Concrete through Ice Recrystallization Inhibition by Poly(vinyl alcohol). ACS Omega, 5(22), 12825–12831. doi:10.1021/acsomega.0c00555.

- [16] Afroughsabet, V., & Al-Tabbaa, A. (2023). Effect of SAPs and polypropylene fibres on the freeze-thaw resistance of low carbon roller compacted concrete pavement. MATEC Web of Conferences, 378, 08006. doi:10.1051/matecconf/202337808006.
- [17] Wathiq Hammodat, W. (2021). Investigate road performance using polymer modified concrete. Materials Today: Proceedings, 42, 2089–2094. doi:10.1016/j.matpr.2020.12.290.
- [18] Saeed, H. H. (2021). Properties of polymer impregnated concrete spacers. Case Studies in Construction Materials, 15, 772. doi:10.1016/j.cscm.2021.e00772.
- [19] Caiyun, W., Li, W., Zhang, C., & Jinpeng, F. (2019). Effect of Protective Coatings on Frost Resistance of Concrete Structures in Northeast Coastal Areas. IOP Conference Series: Materials Science and Engineering, 678(1), 012108. doi:10.1088/1757-899x/678/1/012108.
- [20] Liu, T., Zhang, C., Zhou, K., & Tian, Y. (2021). Freeze-thaw cycling damage evolution of additive cement mortar. European Journal of Environmental and Civil Engineering, 25(11), 2089–2110. doi:10.1080/19648189.2019.1615992.
- [21] Matar, M. G., Aday, A. N., & Srubar, W. V. (2021). Surfactant properties of a biomimetic antifreeze polymer admixture for improved freeze-thaw durability of concrete. Construction and Building Materials, 313, 125423. doi:10.1016/j.conbuildmat.2021.125423.
- [22] Ji, Y., Zou, Y., Ma, Y., Wang, H., Li, W., & Xu, W. (2022). Frost Resistance Investigation of Fiber-Doped Cementitious Composites. Materials, 15(6), 2226. doi:10.3390/ma15062226.
- [23] Gojević, A., Grubeša, I. N., Marković, B., & Filipović, N. (2021). Efficiency of Self-Healing Chemical Additives on the Freeze / Thaw Resistance of Cement Composites. Journal of Innovations in Civil Engineering and Technology, 3(2), 155–168.
- [24] Gojević, A., Netinger Grubeša, I., Juradin, S., & Banjad Pečur, I. (2024). Resistance of Concrete with Crystalline Hydrophilic Additives to Freeze–Thaw Cycles. Applied Sciences (Switzerland), 14(6), 2303. doi:10.3390/app14062303.
- [25] Du, W., Liu, Q., & Lin, R. (2021). Effects of toluene-di-isocyanate microcapsules on the frost resistance and self-repairing capability of concrete under freeze-thaw cycles. Journal of Building Engineering, 44, 102880. doi:10.1016/j.jobe.2021.102880.
- [26] SR 3518:2009. (2009). Tests on Concrete. Determining the Freeze-Thaw Resistance by Measuring the Variation of the Compressive Strength and/or the Relative Dynamic Modulus of Elasticity. Romanian Standards Association (ASRO), Bucharest, Romania.
- [27] ASTM C666/C666M-15. (2024). Standard Test Method for Resistance of Concrete to Rapid Freezing and Thawing (Withdrawn 2024). ASTM International, Pennsylvania, United States.
- [28] GBT 50082 2009. (2009). Standard for Test Methods of Long-Term Performance and Durability of Ordinary Concrete. China Architecture and Building Press, Beijing, China.
- [29] ASTM C666/C666M-03(2008). (2015). Standard Test Method for Resistance of Concrete to Rapid Freezing and Thawing. ASTM International, Pennsylvania, United States. doi:10.1520/C0666\_C0666M-03R08.
- [30] Chen, J., He, Z., Chen, S., Nguyen, P. M. V., Liu, J., & Xu, H. (2025). Study on freeze-thaw damage of surface and pore structure of steam cured concrete. Scientific Reports, 15(1), 22594. doi:10.1038/s41598-025-06958-y.
- [31] CEN/TS 12390-9:2016. (2016). Testing hardened concrete Freeze-thaw resistance with de-icing salts. Scaling. European Committee for Standardization, Brussels, Belgium.
- [32] CEN/TR 15177:2006. (2006). Testing the Freeze-Thaw Resistance of Concrete—Internal Structural Damage. European Committee for Standardization, Brussels, Belgium.
- [33] Zhao, J., Zhang, H., Xu, J., Cui, Y., & Huang, W. (2025). Dynamic Behavior and Damage Mechanisms of Concrete Subjected to Freeze–Thaw Cycles. Buildings, 15(12), 2009. doi:10.3390/buildings15122009.
- [34] Qin, Q., Zheng, S., Li, L., Dong, L., Zhang, Y., & Ding, S. (2017). Experimental Study and Numerical Simulation of Seismic Behavior for RC Columns Subjected to Freeze-Thaw Cycles. Advances in Materials Science and Engineering, 2017, 1–13. doi:10.1155/2017/7496345.
- [35] Kosior-Kazberuk, M., & Wasilczyk, R. (2018). Influence of static long-term loads and cyclic freezing/thawing on the behaviour of concrete beams reinforced with BFRP and HFRP bars. MATEC Web of Conferences, 174, 4013. doi:10.1051/matecconf/201817404013.
- [36] Duan, A., Li, Z. Y., Zhang, W. C., & Jin, W. L. (2017). Flexural behaviour of reinforced concrete beams under freeze–thaw cycles and sustained load. Structure and Infrastructure Engineering, 13(10), 1350–1358. doi:10.1080/15732479.2016.1268172.
- [37] Gong, F., Wang, Z., Xia, J., & Maekawa, K. (2021). Coupled thermo-hydro-mechanical analysis of reinforced concrete beams under the effect of frost damage and sustained load. Structural Concrete, 22(6), 3430–3445. doi:10.1002/suco.202100170.

- [38] Cao, D. F., Zhou, K. F., Zhou, M., Ge, W. J., & Wang, B. Y. (2014). Study on the shear behaviors of RC beams after freeze-thaw cycles. Applied Mechanics and Materials, 488, 750–754. doi:10.4028/www.scientific.net/AMM.488-489.750.
- [39] Chen, C., Zhang, K., & Ye, L. (2024). Influence of Freeze–Thaw Cycles and Sustained Load on the Durability and Bearing Capacity of Reinforced Concrete Columns. Materials, 17(24), 6129. doi:10.3390/ma17246129.
- [40] Liu, X., Tan, W., Ma, E., & Niu, D. (2024). Bond performance of freeze-thaw damaged concrete and reinforcing bars subjected to high-cycle fatigue loading. Construction and Building Materials, 428, 136350. doi:10.1016/j.conbuildmat.2024.136350.
- [41] Yang, M., Xu, Q., Yuan, H., Yang, S., Jiang, Y., Zhang, C., Xu, Y., Su, C., & Zhang, Z. (2025). Bond slip behavior of light steel and foamed concrete under freeze-thaw cycles. Scientific Reports, 15(1), 18077. doi:10.1038/s41598-025-03366-0.
- [42] Cao, D. F., Ge, W. J., Wang, B. Y., & Tu, Y. M. (2015). Study on the flexural behaviors of RC beams after Freeze-Thaw cycles. International Journal of Civil Engineering, 13(1), 92–101. doi:10.22068/IJCE.13.1.92.
- [43] Kim, S., Lee, Y., Kim, J., & Han, D. (2025). Influence of Air Content on the Behavior of RC Beams Subjected to Freezing and Thawing. International Journal of Concrete Structures and Materials, 19(1), 12. doi:10.1186/s40069-024-00746-0.
- [44] Omran, H., & El-Hacha, R. (2014). Effects of sustained load and freeze-thaw exposure on RC beams strengthened with prestressed NSM-CFRP strips. Advances in Structural Engineering, 17(12), 1801–1816. doi:10.1260/1369-4332.17.12.1801.
- [45] EN 1097-6:2013. (2013). Tests for mechanical and physical properties of aggregates. Part 6, Determination of particle density and water absorption. European Committee for Standardization, Brussels, Belgium.
- [46] EN 196-6:2019. (2019). Methods of testing cement Part 6: Determination of fineness. European Committee for Standardization, Brussels, Belgium.
- [47] ISO 9277:2010. (2010). Determination of the specific surface area of solids by gas adsorption BET method. International Organization for Standardization (ISO), Geneva, Switzerland.
- [48] EN 1992-1-1:2023. (2023). Eurocode 2. Design of concrete structures General rules and rules for buildings, bridges and civil engineering structures. European Committee for Standardization, Brussels, Belgium.
- [49] EN 12390-3:2019. (2019). Testing hardened concrete Compressive strength of test specimens. European Committee for Standardization, Brussels, Belgium
- [50] FEMA 461. (2007). Interim Testing Protocols for Determining the Seismic Performance Characteristics of Structural and Nonstructural Components. Applied Technology Council, Redwood City, United States.
- [51] Park, S., Zeng, H., Kim, H. J., & Kundu, T. (2025). Evaluation of freeze-thaw effect on concrete using sideband peakcount-based non-linear ultrasonic NDT&E techniques. Structural Health Monitoring. doi:10.1177/14759217241310162.